Title
TWO-PHASE MICROSTRUCTURES OF a -Fe-Al ALLOYS IN THE K-STATE

Authors
Warlimont, H.
Thomas, G.

Publication Date
1969-02-01

Submitted to Physica Status Solidi

UCRL-18610
Preprint

TWO-PHASE MICROSTRUCTURES OF α-Fe-Al ALLOYS IN THE K-STATE

H. Warlimont and G. Thomas

February 1969

AEC Contract No. W-7405-eng-48

LAWRENCE RADIATION LABORATORY
UNIVERSITY of CALIFORNIA BERKELEY

UCRL-18610

DISCLAIMER

UCRL-18610

TWO-PHASE MICROSTRUCTURES OF α-Fe-Al ALLOYS IN THE K-STATE

H. Warlimont* and G. Thomas

Inorganic Materials Research Division, Lawrence Radiation Laboratory, Department of Materials Science and Engineering, University of California, Berkeley, California

ABSTRACT

Electron diffraction and microscopy have been utilized to investigate the Fe-Al system up to 20 at.% Al. It is found that alloys at and above 10 at.% Al aged at low temperatures consist of two phases as indicated by coherent particle strain contrast images and by electron diffraction. At 18 at.% Al and above the particles are identified as the α_1 phase exhibiting DO_3 type structure. Thus, the so-called K-state and other abnormal properties attributed previously to short range order in these alloys are associated with very small ordered particles (50Å or less in diameter). Outside the conventional two-phase field growth of these particles is severely limited.

*Permanent Address: Max-Planck-Institut fur Metallforschung, Institut fur Metallkunde, Stuttgart, Germany.

INTRODUCTION

Iron-aluminium solid solutions 5 to 19% Al* exhibit an increase in electrical resistivity when quenched and aged, and a decrease when quenched and deformed. [1,2] This abnormal behavior is not observed in pure metals and most dilute alloy solid solutions, but has been found in numerous concentrated alloy solid solutions, has been called the "K-state". [3] Further investigations of pertinent Fe-Al alloys have shown that aging of quenched states results in up to 0.03% volume contraction, formation of broad x-ray superlattice reflections compatible with the DO_3 structure, and an increase of up to 25% in the 0.05% proof stress. [4] Some authors have ascribed these effects to the occurrence of short range order or clustering, whose physical nature has not been revealed, however.

It is useful to relate the observations pertaining to short range order to the constitution of the alloys as given in the phase diagram. The iron-rich part of the Fe-Al system has been revised recently based on electron microscopic observations and on a re-evaluation of published data. [5,6] The equilibria in the range of temperatures and compositions pertinent to the present study are shown in Fig. 1. Anomalous changes of physical and mechancial properties have been observed in the shaded region marked A, as well as in the Fe-rich part of the $\alpha + \alpha_1$, two-phase region. [1,2,4]

In this investigation, Fe-Al alloys have been studied by electron microscopy and electron diffraction because it has been shown that these methods are well suited to yield information on the structural nature of short range ordered alloys [7-9] which cannot be derived from measurements of bulk physical properties.

---

*All compositions are given in atomic per cent.

While this investigation was underway, D. Watanabe et al. [10] have published some pertinent electron microscopic observations. The authors interpret their micrographs to indicate that the "K-state" in Fe-Al alloys containing 19.60 and 20.02% Al is related to the inhomogeneous formation of small "domains"* of DO_3 type structure. These authors suggest that the maximum in resistivity corresponds to a critical domain diameter d_m <50Å. They did not distinguish, however, between alloys in region A and in the $\alpha + \alpha_1$ two-phase field.

EXPERIMENTAL PROCEDURES

Alloys containing 1, 9.9, 15.5, 17.8, 18.7, and 20.5 at. % Al were chosen for this investigation in order to cover the α solid solution and region A exhibiting anomalous behaviour, as well as the conventional $\alpha + \alpha_1$ two-phase field. The metals of 99.99% purity were induction melted under 100 torr He pressure and chill-cast into copper moulds. The alloys were rolled at 1000° to 1100°C into strips 0.3mm thick, which were re-heated after each pass. Samples of these strips were used for wet chemical analysis whose results were accurate to within $\pm$ 0.2 at. % Al. All specimens to be investigated microscopically were first sealed in quartz tubes filled with He to give a pressure of 760 torr at the annealing temperature. They were annealed for about one hour at 1380°C and quenched in water by cracking the tubes immediately after submerging them. The specimens were then sealed in glass tubes filled with He and aged for different times at 200°, 250°, and 300°C. Some specimens were cold-rolled to approximately 5% elongation prior to the aging treatment. Thin foils for electron microscopic investigation were prepared by electro-polishing using the Bollmann technique.

*In this paper regions of order in a disordered matrix are called "particles", whereas contiguous regions of order which are antiphase to one another are called "domains".

The electrolyte consisted of 1 part nitric acid and 2 parts methyl alcohol. Polishing conditions were: 5 to 6 V, -5 to -15°C.

RESULTS

The alloys examined in this investigation, which lie within the region marked A in Fig. 1, showed contrast effects ("tweed patterns") in bright-field and dark-field images of (fundamental) reflections which can be interpreted in terms of a profusion of weak localized strain fields with an overall alignment predominantly in ⟨110⟩, but also in ⟨100⟩ depending on the foil normal and on the operating reflection. Similar effects have been observed, e.g., during ordering in Nb-O [11], Ta-C [12], and during precipitation in Cu-Be [13]. These features, as well as diffuse diffraction phenomena, are illustrated in Figs. 2-4. Such effects are not observed in pure iron nor in Fe-1% Al and are not artefacts resulting from specimen preparation. The results can be explained, however, if precipitation of coherent particles has occured. In the latter case, under appropriate conditions of imaging, coherent particles are expected to show strain contrast images if the strain fields are strong enough and when $\vec{g}.\vec{R} \neq 0$, where $\vec{g}$ is the operating diffraction vector and $\vec{R}$ is the displacement vector associated with the particle. When individual particles are resolved (as in Fig. 4c), the two beam dynamical theory can be applied to interpreting the nature of the particles from the appearance of the strain contrast images, e.g., the intensity distribution of the black-white contrast lobes with respect to the direction of $\vec{g}$ [14-16]. However, complications can occur [15] when the volume fraction of particles is so high that strain fields overlap, and when the particles are too small to be individually resolved (as in Fig. 2).

When the strain contrast is considered in detail it becomes impossible to interpret the images in terms of simple displacements [14-16]. For example,

Figs. 2a-e indicate that there is no unique relationship between the strain contrast images and the direction of the diffraction vector $\vec{g}$. In regions where particles can be resolved, the black-white images typical of coherent particles with strain fields around them are sometimes parallel to, normal to, or at an angle to $\vec{g}$ (see Figs. 2b, c and Fig. 4c). This means that particles cannot be clearly distinguished as being spherical, disc-shaped, nor rod-like [15]. Similar difficulties in identification have been encountered in specimens containing very large numbers of small point defect clusters, e.g., after quenching or irradiation (see e.g., Ref. 16). Another difficulty in resolving particles is associated with the weakness of the strain contrast images (compare the matrix strain fields with those due to dislocations in Figs. 2a, b).

Up to Fe-18% Al there was no change in the type of image from those shown in Fig. 2, neither when the composition was changed nor when the time of heat treatment was varied (aging ranged up to periods of one week at 200° and 300°C respectively). That is, it was not possible to coarsen the structure by particle growth thus enabling individual particles to be resolved. Particles could only be resolved in alloys containing more than 18% Al as is shown in Fig. 4. Even though in Fig. 4a particles can be seen in the dark-field image of the superlattice reflections, now resolved in diffraction patterns (Fig. 3g), the corresponding bright-field images are not different from those in Fig. 2. However, when alloys within the conventional two-phase ($\alpha + \alpha_1$) field are observed, e.g., Fe-20% Al (Fig. 4b, c), particle growth can be accomplished and strain contrast images are more clearly resolved.

When the particles themselves can be directly imaged, viz., when superlattice reflections are observed and their dark-field images can be obtained

(Fig. 4), they are not regular but appear roughly isometric in shape. Their sizes vary up to about 100Å; these particles are the α_1 phase, i.e., Fe_3Al [5,6].

All of these results indicate that the shape of the particles is adapted on precipitation to accomodate strains. Whilst the transformation $\alpha \rightarrow \alpha_1$ is cubic to cubic and the strains are thus purely dilational, due to the anisotropic nature of this alloy, an isometric particle shape is not realized. A complex shape adapting to the strain energy relief as well as to interfacial energy restrictions is thus not unexpected.

A similar situation exists in Cu-Be alloys [13] when discs have precipitated in {100}. Strain patterns in $\langle 110 \rangle$ are observed due to $\{110\}\langle 1\bar{1}0 \rangle$ shear strains when the volume fraction is so large that strain fields overlap. In the Fe-Al alloys, it may be similarly concluded that the strain patterns observed are due to overlapping $\{110\}\langle 1\bar{1}0 \rangle$ shear strain fields as a result of a very large volume fraction of small particles. A large volume fraction of precipitate appears to be essential for the described shear strains to arise [13a]. In these cases, strain contrast theory as presently developed for individual strain centers [14-16] is no longer applicable.

In analysing the alignment of image contrast as a function of foil orientation and operating reflection, it is found that most images exhibit striations along $\langle 110 \rangle$ (e.g., Figs. 2a, 2c), in some images no alignment is clearly distinguishable (e.g., Fig. 2d), but with an [001] foil normal and $\vec{g} = 200$ (as in Fig. 2b) individual centers of contrast can be recognized whose overall alignment is along [100] and [010]. We conclude that this pattern corresponds to the actual alignment of the particles. The appearance of the contrast in Fig. 2b can arise from overlapping displacements

as a result of combinations such as $\vec{R} = [1\bar{1}0] \pm [110]$. Such effects are expected to be strongest in [001] foils such as shown in Fig. 2b.

The above considerations are also supported by the electron diffraction patterns (Fig. 3), which show the following effects: All specimens produce "short range" streaking in directions close to $\langle 110 \rangle$ and $\langle 211 \rangle$ which is observed most strongly at slight deviations from low-index zones. Sometimes diffuse streaking in these directions is extending from relpoint to relpoint, Fig. 3b; this "long range" streaking is found in freshly quenched specimens and also in alloys within the conventional two-phase field (~19% Al - 25% Al), Fig. 3 . At 15.5% Al and above superlattice reflections of the DO_3 structure are resolved, Figs. 3c, 3e-g.

The "short range" streaks observed in the diffraction patterns (Fig. 3) are probably due to the elastic strains set up by the ordering transformation. This may be deduced from the facts, that these streaks were not observed at the origin and that their length increases with increasing order of the reflection. Shape factor streaks which are produced as a consequence of relaxation of Laue conditions due to particles of small dimensions may also be present. The more continuous streaks seen predominantly in diffraction patterns from freshly quenched foils (Fig. 3b) could indicate very small plate-like (or rod-like) particles which grow on aging to a rather more isometric shape.

From these observations, we conclude that in alloys within the region A of Fig. 1, two phases, one disordered (α) and one ordered (α_1) are present; but, the particle size of the ordered phase is too small to be clearly resolved in alloys containing less than about 18% Al. The results give no indication of the degree of order in the α_1 particles. As shown in Fig. 4, direct evidence of the presence of ordered particles may only be obtained

from appropriate dark-field images of diffuse, or superlattice reflections. The observation of strain fields is the only way of deducing that alloys contain two phases when non-fundamental reflections are not resolved or have insufficient intensity. The appearance of superlattice reflections may be correlated with precipation of α_1 which has reached a volume fraction and degree of order sufficient to produce visible superlattice reflections at about 15.5% Al. This is in accord with X-ray investigations by Davies who found broad α_1 superlattice lines at 17.9% Al [4].

The amount of strain resulting from the transformations may be estimated from the difference in lattice parameter of the two phases if it is assumed that the pertinent two phase field consists of region A and the conventional $\alpha + \alpha_1$ region. Based on this assumption, the composition of α is $\sim$10% Al, whilst that of α_1 is 25% Al at 300°C. From the lattice parameter data of Taylor and Jones [17], the strain is found to be $\varepsilon = 2(a^{\alpha} - a^{\alpha 1})/(a^{\alpha} + a^{\alpha 1}) \sim 0.5\%$, which is small compared to strains arising during precipitation in systems such as Al-Cu [18] and Cu-Be [13]. This small strain accounts for the weakness of the strain contrast images, Fig. 2. The particle size must exceed a certain value for the effect to be observed at all.

In the specimens containing incipicient precipitation after quenching, which had been cold-rolled prior to aging, dislocations were observed to be uniformally distributed, i.e., cell-formation was not detected. At 20.5% Al, the dislocation lines are predominantly straight and parallel to $\langle 111 \rangle$ directions, Fig. 5. This alignment was found to be less pronounced the lower the Al content.

DISCUSSION

Microstructural Observations

The electron microscopic observations have shown that a fine dispersion of particles, i.e., a two-phase microstructure is present in all Fe-Al alloys heat treated in (or quenched into) region A as well as in the conventional $\alpha + \alpha_1$ two-phase field as delineated in Fig. 1.* The particle arrangement, size and shape can be estimated from indirect evidence even though the particles cannot be resolved individually by the methods employed in this investigation, until the Al content is equal to or greater than 18%.

Below 18% Al where the particles can only be observed by strain contrast, it may be derived from the image contrast such as in Fig. 2b, that no dimension of an individual particle is longer than the average particle spacing. However, if the phases present in region A are referred to a two-phase field comprising region A and the conventional $\alpha + \alpha_1$ region, the strain due to the difference in lattice parameters referred to 300°C is $\varepsilon \leq 0.5\%$ as derived above. This comparatively low value leads to isometric particle shapes in Ni-Al alloys [20] where particles up to d = 100Å in diameter were found to be isometric if $\varepsilon \leq 0.5\%$. In the present case, however, the strain contrast in the images and the streaks due to directional strains in the diffraction patterns indicate that considerable anisotropic strains prevail. This anisotropy is related to the pronounced elastic anisotropy $A = 2C_{44}/(C_{11} - C_{12})$ of Fe-rich Fe-Al alloys [21] which ranges from A (10 at. % Al) = 3.2 to A (25 at. % Al) = 6.5 at room temperature.

These relatively high values (compare to A (Al) = 1.2, A (Fe) = 2.4, A (Ni) = 2.5) suggest that the particle shape may not be spherical because

---

*In this context the term particle is chosen as a convenient way of describing the observed diffraction effects. It is realized, that the existence of finite gradients of concentration and degree of order in the interfaces cannot be excluded nor proved in the present work.

of configurational stress minimization. This conclusion is supported by the observation of 110 strain maxima in Cu-Be alloys containing coherent precipitates on {001} [13] where this effect may be uniquely related to a high value of the elastic anisotropy. Alternatively the observed strain contrast can equally well be explained as due to overlap of individual particle strain fields when the volume fraction is very large.

The particle size in region A may be assessed on the assumption that region A and the conventional $\alpha + \alpha_1$ region are the effective $\alpha + \alpha_1$ two-phase field. The volume fraction of the α_1-phase $f^{\alpha 1}$ is then given by $f^{\alpha 1} = (c^o - c^\alpha)/(c^{\alpha 1} - c^\alpha)$, where c^o, c^α, and $c^{\alpha 1}$ give the Al-concentrations of the alloy and of the phases, respectively, If the particle spacing is D, the particle diameter $d = D(f^{\alpha 1})^{1/3}$. From counts on 11 micrographs of alloys containing 15.5 to 17.8% Al and held at 300°C for different times the average lateral distance of strain centers was found to be $100 < D < 200$Å irrespective of composition and aging time. If this observed value is taken to correspond to the average particle spacing we obtain with $f^{\alpha 1} = 0.33$ (viz. Fig. 1), the particle diameter to be $70 < d < 140$Å. It will be discussed further below that this value is to be considered as a theoretical upper limit of the actual particle diameter.

The exact nature of the short range ordered state has not been uniquely established in general. Two different models are commonly utilized, a) a statistical model, b) a subdivision of the long range ordered state into small antiphase domains (see e.g., Refs. 22, 23). The present results indicate that the short range ordered state is different from both models consisting of very small ordered particles in a disordered α-matrix. At 18% Al and above, the particles are resolved and identifyable as α_1. Although the diffraction patterns from alloys below approximately 15.5% Al

do not show diffuse scattering effects other than those arising from strains, it is reasonable to suppose that particles in such alloys are also α_1 but within which there may be a variable degree of order depending on composition and heat treatment. Similar evidence for the particle nature of the SRO state has been found by Ruedl et. al. [24] in Ni_4Mo, and one can interpret the results of Blackburn [25] on Ti-Al in like manner. However, these results were obtained from alloys quenched from above T_c when the possibility of incipient ordering exists. That is, it may be questionable to suppose that quenched alloys retain the actual short range ordered condition existing above T_c. Tanner et. al [26] working on Au-Mn and Au-Cr using high temperature electron diffraction (but with no dark-field imaging) obtained results on short range order, at temperature, which contradict the microdomain concept if the latter is considered to be merely small regions of normal long range order. However, recent work on Ni_4Mo by Okamoto and Thomas (to be published) has resolved this discrepancy and gives added support to the two-phase particle model of SRO.

Correlation with Previous Observations

Region A of the Fe-Al alloy system has been studied prior to this work by resistivity, [1,2] dilatometric, [2,4] X-ray [4] and flow stress [4] measurements which will now be discussed in relation to the present observations.

The anomalous increase in resistivity which H. Thomas [3] has called the K-state has been observed not only in Fe-Al alloys, [2,3,4], but also in numerous other alloy systems (quoted in Refs. 2-4, 27, 28). Until recently the K-state has been attributed to an enhanced scattering when small particles have a size comparable with the wavelength of the conduction electrons [29]. Since in Al alloys this wavelength is too small an alternate explanation in

terms of Umklapp-scattering was devised [30] and was found to yield a quantitative rationalization of the experimental observations on Al alloys [31, 32] where the maximum in resistivity corresponds to $d_m \approx 15 \pm 5$Å. Recently, a theory based upon Bragg scattering from clusters (e.g., G. P. zones) has been proposed [33, 34] which may be supported by the present observations. It should be emphasized in this context that the K-state is observed in so-called short range ordered states as well as during the early stages of other precipitation processes. This indicates that short range order is characterized by the presence of discrete second-phase particles of a particular size or size distribution.

It should be noted, however, that in the K-state, the total scattering of conduction electrons depends not only on the particle size, but also on further parameters such as the volume fraction of scattering particles, the crystal structures of the matrix and the particles, strain fields, and the temperature of measurements. Therefore, the relations between resistivity and particle size in alloys in the K-state do not follow a simple functional relationship. For most systems they can only be assessed empirically and qualitatively at present.

The results of resistivity measurements on Fe-Al alloys in the range of the present investigation may be summarized as follows: Upon isothermal aging, the resistivity changes correspond to those characteristic of a property whose magnitude depends on particle size [2]; the rate of increase in resistivity with time increases continuously across the boundary between region A and the conventional $\alpha + \alpha_1$ two-phase field with increasing Al concentration; the increase is particularly pronounced above ~19% Al [2]; the steady state resistivity of an alloy at any one temperature in region A is independent of its thermal history [1]; plastic deformation decreases

the resistivity of quenched alloys (deformation and measurements at room temperature) above 4% Al [1]; the decrease in resistivity due to plastic deformation reaches a constant value if the strain $\leq$ 50% [1]; isothermal aging of deformed alloys results in essentially the same resistivity changes as those occuring in as-quenched alloys [1].

The present results combined with the results of the resistivity measurements may be rationalized as follows: In all alloys with more than about 4% Al, quenching to room temperature results in the nucleation and incipient growth of α_1 particles. Upon aging, these particles are revealed by electron microscopy through strain contrast. When passing through a critical range of sizes during growth, they cause an increase in electrical resistivity (above that of a random solid solution) due to the K-effect. These particles may be destroyed by plastic deformation resulting in a decrease in resistivity. If the particles are allowed to grow by isothermal annealing, they reach a constant volume fraction. Moreover, they reach an equilibrium size when annealed in region A, while they are subjected to continuous coarsening when annealed in the conventional $\alpha + \alpha_1$ two-phase field. These conclusions may be drawn from direct observation as well as from the fact that resistivity changes in region A lead reversibly to steady state values.

The equilibrium size and volume fraction of α_1 particles in region A depend on the Al concentration and aging temperature. This is reflected by the present observations as well as by the resistivity measurements which indicate, that the K-effect increases with increasing Al concentration [1,13] and decreasing aging temperature. [1] A quantitative correlation is not possible due to the variation in the temperature coefficient of resistivity with the state of precipitation [2] and the lack of sufficient accuracy in

direct observations.

Dilatometric measurements have shown that quenched specimens contract upon subsequent aging, [4] and that the rate of contraction during isothermal aging decreases continuously until a final value is reached, while the resistivity of the same specimen passes through a maximum [2].

The contraction of quenched alloys upon aging in region A is due to the decrease of the Al concentration accompanied by a decrease in lattice parameter [17] of the α phase during precipitation of the (assumed) α_1 phase. The decrease is, however, compensated for in part by the α_1 phase which has a larger lattice parameter than the average parameter of alloys below 19% Al.

The X-ray observations [4] have shown that quenching of an alloy containing 17.9% Al, i.e., in the range of region A results in the development of one broad maximum of diffuse scattering, while aging produces rather broad superlattice reflections of the DO_3 structure exhibiting increasing intensity with decreasing aging temperature. These results are compatible with incipient growth of α_1 particles during quenching and an increasing amount of α_1 phase to be formed with decreasing aging temperature. In view of the present results, the broadness of the X-ray reflection is interpreted to be due to small particle size as well as to strain fields.

The increase in flow stress due to annealing of an alloy containing 16.5% Al in region A [4] was originally ascribed to the presence of a very small domain size [4]. The present results show, however, that the effect is due to dispersion strengthening by coherent particles as in systems such as Al-Cu, [18], Cu-Be, [13].

GENERAL CONCLUSIONS

The present findings in combination with the results of previous investigations indicate that the actual $\alpha + \alpha_1$ two phase field in Fe-Al alloys comprises region A as well as the conventional $\alpha + \alpha_1$ region as shown in Fig. 1. In support of this interpretation it may be pointed out that the boundary of region A when extrapolated extends approximately to the tie line of the eutectoid reaction $\alpha_2 \rightleftarrows \alpha + \alpha_1$ and to 0% Al at 0°K. The latter is hardly realized for the conventional $\alpha/\alpha + \alpha_1$ phase boundary. However, whereas the particle size is not limited in the conventional $\alpha + \alpha_1$ region, it appears to be approaching an equilibrium value at any given composition and temperature in region A. Thus, it appears that the particle growth in region A is not impeded for kinetic, but for thermodynamic reasons. If this is the case, the free energy relations must depend on strain effects in relation to the particle size in such a way that a minimum in free energy of the system is obtained for a particular dispersion of particles. If this interpretation is accepted, it follows that the lever rule as applied to the conventional free energy v.s. concentration curves for deriving the volume fractions of the phases is not applicable in region A. The free energy functions would rather have to be modified to incorporate a strain energy term and other terms related to the stable dispersion of particles, e.g., to their quasi-periodic array. Consequently, the particle size and the strains arising during transformation, which have been derived above taking the boundary of region A as a conventional phase boundary will only give the theoretical upper limit of these quantities.

Thus, it is concluded that the range of what has been termed short range order in the Fe-Al system up to now, is actually part of a two-phase field $\alpha + \alpha_1$, but within this field two regions may be discerned where the

stability of the α and α_1 phases is a function of different variables. Corresponding observations were made in the Cu-Al system [35]. This suggests that a general principle may be involved and may require a reconsideration of the present concepts of short range order.

ACNOWLEDGEMENTS

We wish to thank the United States Atomic Energy Commission for continued financial support and for making this collaboration possible at Berkeley. We also thank Miss M. Robson and D. Jurica for help with the experimental work.

REFERENCES

[1] H. Thomas, Z. Metallkde., 41, 185 (1950).

[2] H. Saito and H. Morita, J. Japan Inst. Met., 30, 930 (1966).

[3] H. Thomas, Z Physik, 129, 219 (1951).

[4] R. G. Davies, J. Phys. Chem. Solids, 24, 985 (1963).

[5] G. Lutjering and H. Warlimont, Z. Metallkde., 56, 1 (1965).

[6] H. Warlimont, to be published in Z. Metallkde.

[7] K. Sato, D. Watanabe, and S. Ogawa, J. Phys. Soc. Jap., 17, 1947 (1962).

[8] D. Watanabe and P. M. J. Fisher, J. Phys. Soc. Jap., 20, 2170 (1965).

[9] D. Watanabe, J. Phys. Soc. Jap., 14, 436 (1959).

[10] D. Watanabe, H. Morita, H. Saito, and S. Ogawa, J. Phys. Soc. Jap., 25, 293 (1968).

[11] L. I. Van Torne and G. Thomas, Acta Met., 12, 601 (1964).

[12] R. E. Villagrana and G. Thomas, Phys. Stat. Solidi, 9, 499 (1965).

[13] L. E. Tanner, Phil. Mag., 14, 111 (1966).

[13a] L. E. Tanner, Phys. Stat. Solidi, in press.

[14] M. F. Ashby and L. M. Brown, Phil. Mag., 8, 1083, 1649 (1963).

[15] W. L. Bell, D. M. Maher, and G. Thomas, Nature of Small Defect Clusters, HMSO, 314 (1966).

[16] M. Rühle, Phys. Stat. Solidi, 19, 263 (1967).

[17] A. Taylor and R. M. Jones, J. Phys. Chem. Solids, 6, 16 (1958).

[18] See e.g., A. Kelly and R. B. Nicholson, Precipitation Hardening, Prog. Mat. Sci., 10, 149 (1963).

[19] H. J. Leamy and H. Warlimont, to be published.

[20] E. Hornbogen and M. Roth, Z. Metallkde., 58, 842 (1967).

[21] H. J. Leamy, E. D. Gibson, and F. X. Kayser, Acta Met., 15, 1827 (1967).

[22] J. M. Cowley, J. Austr. Inst. Met., 11, 258 (1966).

[23] S. C. Moss and P. C. Clapp, Phys. Rev., 171, 754, 764 (1968).

[24] E. Ruedle, P. Delavignette and S. Amelinckx, IV Europ. Conf. Electron Mic., Rome 1968, Vol. 1, p. 311.

[25] M. J. Blackburn, Trans. AIME, 239, 1200 (1967).

[26] L. E. Tanner, P. C. Clapp, and R. S. Toth, Mat. Res. Bull., 3, 855 (1968).

[27] E. Hornbogen and H. Kreye, Z. Metallkde., 57, 122 (1966).

[28] E. A. Starke, V. Gerold, and A. G. Guy, Acta Met., 13, 957 (1965).

[29] N. F. Mott, J. Inst. Met., 60, 267 (1937).

[30] R. Labusch, Phys. Stat. Sol., 3, 1661 (1963).

[31] C. Panseri and T. Federighi, Acta Met., 8, 218 (1960).

[32] T. Federighi and L. Passari, Acta Met., 7, 422 (1959).

[33] P. Wilkes, Acta Met., 16, 863 (1968).

[34] P. Wilkes and A. Hillel, Proc. Manchester Conf. on Phase Transformations, (1968)

[35] H. Warlimont and W. Gaudig, to be published.

FIGURE CAPTIONS

Fig. 1 - Part of the Fe-Al phase diagram showing the region of interest in this investigation. The region A is delineated as the range over which anomalous property changes occur.

Fig. 2 - Strain contrast effects in α-Fe-Al alloys.

(a) Fe - 15.5% Al aged one week at 300°C, bright-field image, $\vec{g} = \bar{1}10$, image normal near [115].

(b) As (a), dark-field of $\vec{g} = 200$, foil normal tilted from [001] towards [013].

(c) As (a), dark-field of $\vec{g} = [1\bar{2}1]$, after tilting to near [111] orientation.

(d) Fe - 15.5% Al aged 1 hr. at 300°C, dark-field, $\vec{g} = 110$, image normal [111].

(e) Fe - 9.9% Al dark-field image using 110 reflection.

Fig. 3 - Electron diffraction patterns of α-Fe-Al alloys.

(a) Fe- 9.9% Al aged one week at 200°C.

(b) 15.5% Al as quenched.

(c) Fe - 15.5% Al aged one week at 300°C, very weak and diffuse 100-superlattice reflections, [001] orientation.

(d) As (c) showing [111] zone, notice diffuseness and asymmetry of spots and diffuse streaks in ⟨112⟩.

(e) Fe - 17.8% Al aged one week at 300°C (compare to Fig. 3f).

(f) Fe - 20.5% Al aged 1 hr. at 300°C, [001] zone, showing ⟨110⟩ streaks and DO_3 superlattice reflections.

(g) Selected area diffraction pattern corresponding to Fig. 4a; [001] orientation.

Fig. 4 - Resolution of the two-phase structure in Fe-Al alloys.

(a) Fe - 18.7% Al aged one week at 300°C. Dark-field of 100 (DO_3) superlattice reflection showing α_1 particles (bright) in disordered α matrix.

(b) Fe - 20.5% Al aged one week at 300°C. Dark-field of 111 (DO_3) superlattice reflection.

(c) Fe - 20.5% Al aged one week at 300°C, foil tilted off [112] for two-beam $\vec{g} = 2\bar{2}0$ dark-field. Strain contrast images from individual particles are resolved. The lines separating the black-white contrast maxima lie parallel to mainly {110} traces indicating displacements in $\langle 110 \rangle$. This gives rise to $\langle 110 \rangle$ streaks in diffraction patterns such as Fig. 3d.

Fig. 5 - Microstructure of a specimen cold-rolled 5% prior to aging for one week at 300°C. Fe - 20.5% Al. Dislocations aligned in $\langle 111 \rangle$ (bright-field).

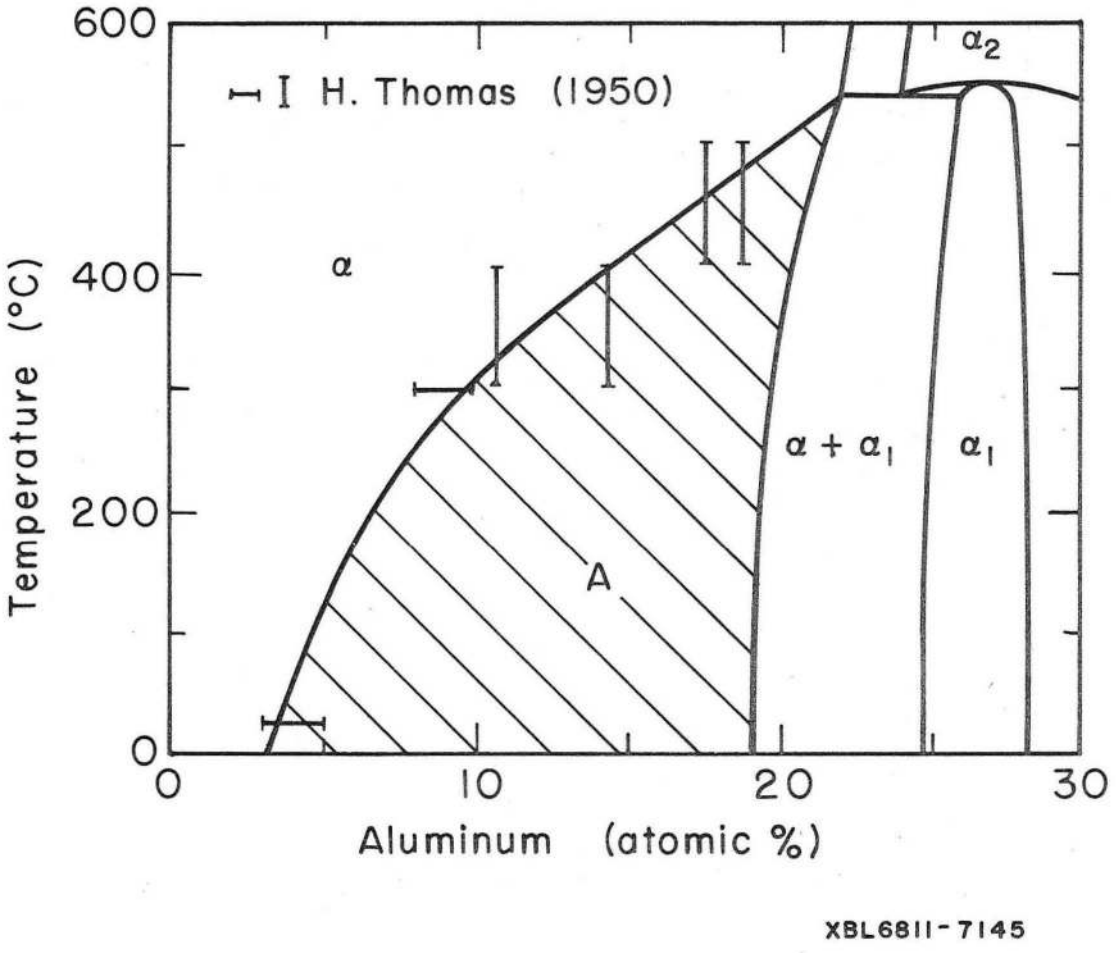
600
400
200
0
Temperature (°C)
H. Thomas (1950)
α
α2
α + α1
α1
A
0
10
20
30
Aluminum (atomic %)
XBL6811-7145

Fig. 1

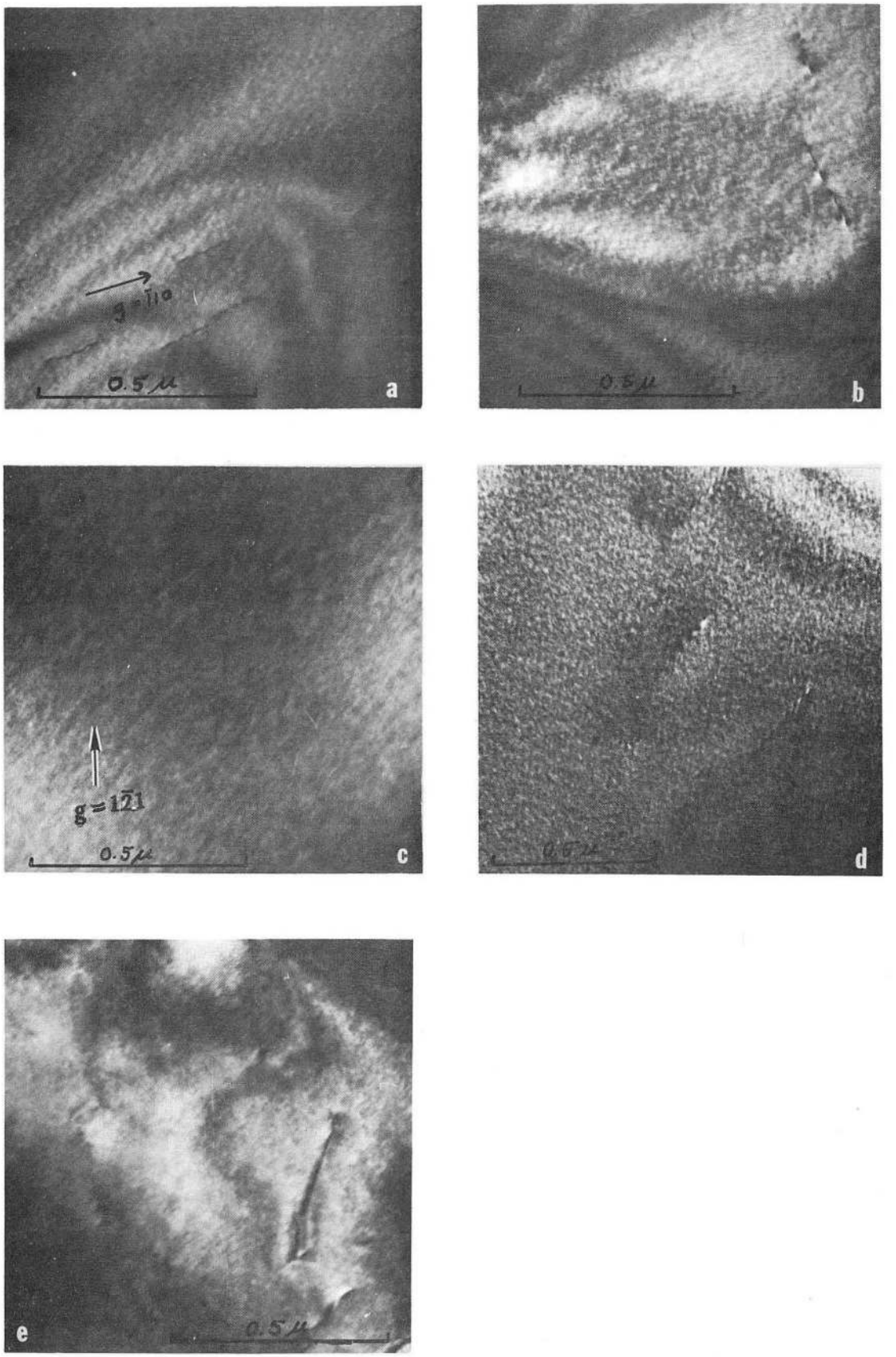

XBB 699-6116

Fig. 2

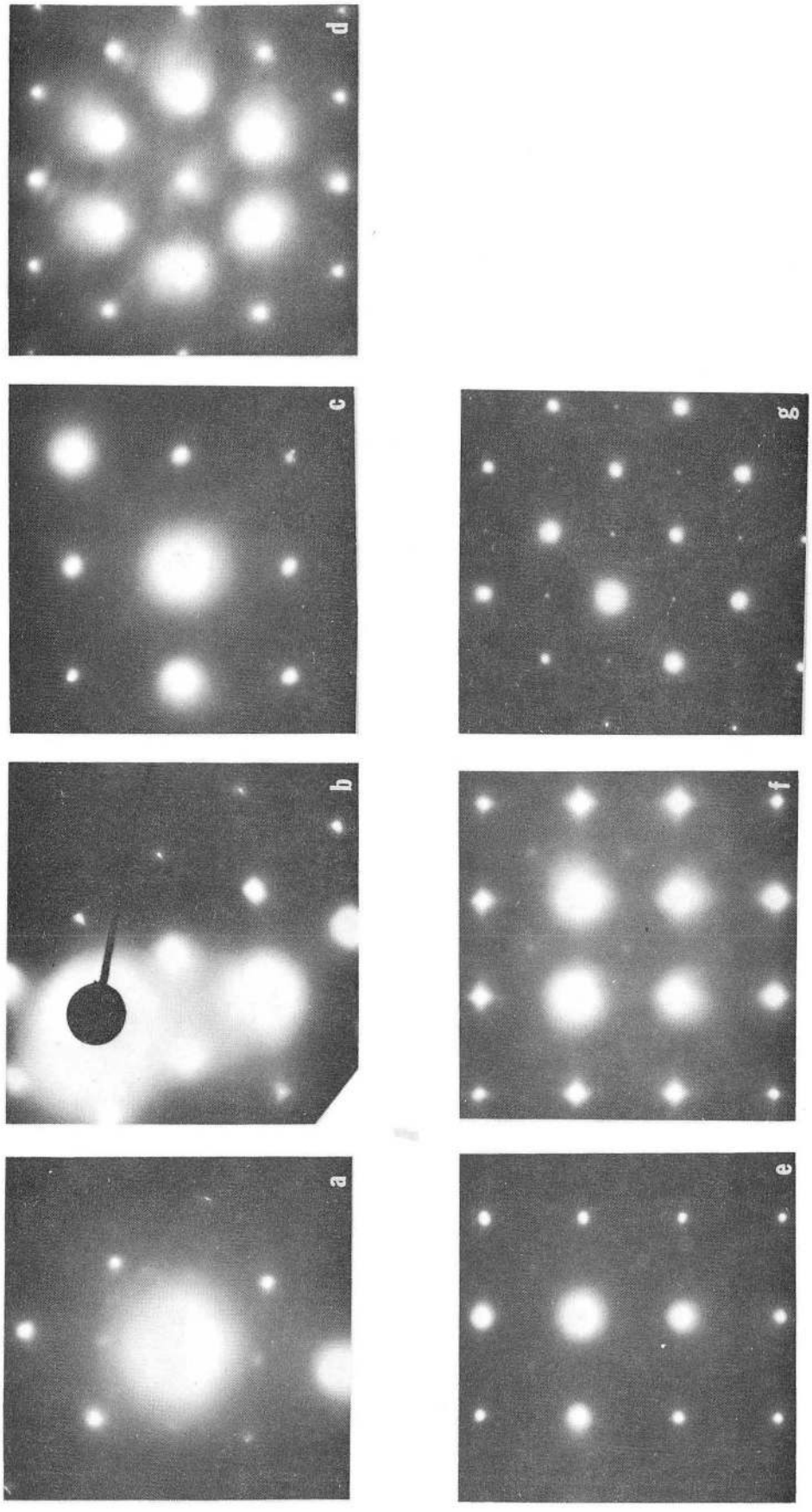

XBB 699-6117

Fig. 3

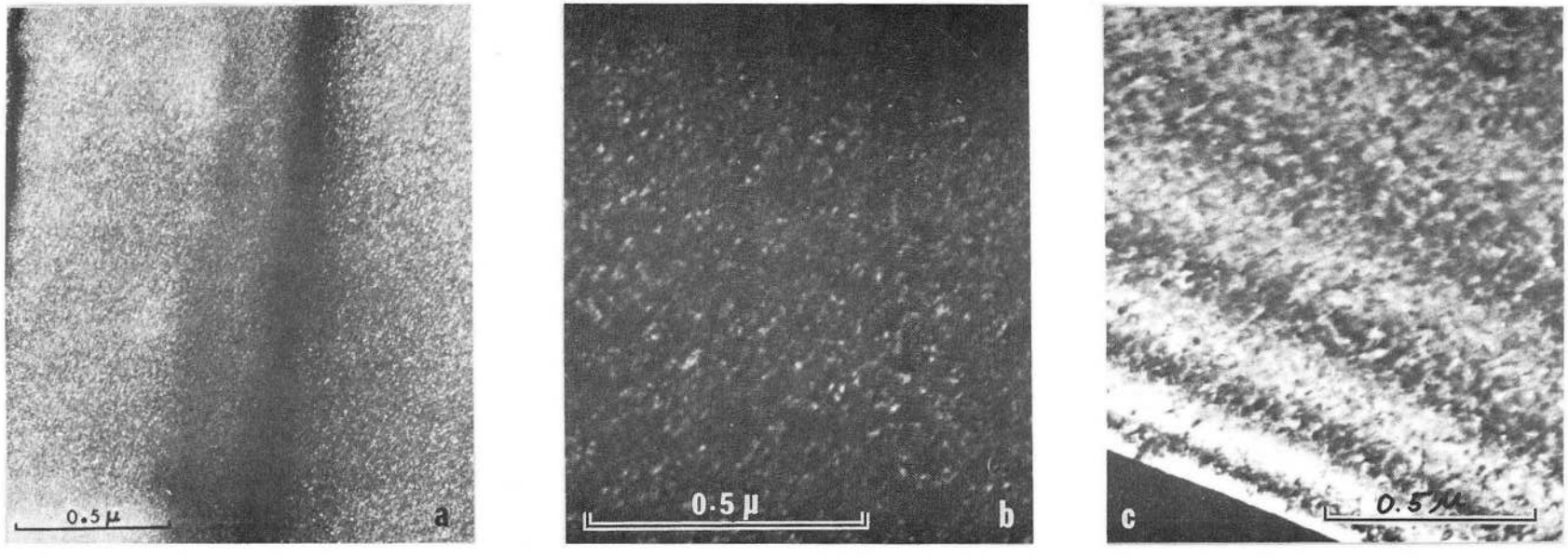

XBB 699-6118

Fig. 4

XBB 699-6119

Fig. 5

TECHNICAL INFORMATION DIVISION
LAWRENCE RADIATION LABORATORY
UNIVERSITY OF CALIFORNIA
BERKELEY, CALIFORNIA 94720